Reductive dissolution of jarosite by inorganic sulfur compounds catalyzed by Acidithiobacillus thiooxidans

Chen, H-R., Zhang, D-R., Nie, Z-Y., Xia, J-L., Li, Q., Zhang, R-Y., Yin, H-H. & Pakostova, E

Original citation & hyperlink:
Chen, H-R, Zhang, D-R, Nie, Z-Y, Xia, J-L, Li, Q, Zhang, R-Y, Yin, H-H & Pakostova, E 2022, 'Reductive dissolution of jarosite by inorganic sulfur compounds catalyzed by Acidithiobacillus thiooxidans', Hydrometallurgy, vol. 212, 105908.
https://doi.org/10.1016/j.hydromet.2022.105908

DOI 10.1016/j.hydromet.2022.105908
ISSN 0304-386X
ESSN 1879-1158

Publisher: Elsevier

Reductive dissolution of jarosite by inorganic sulfur compounds catalyzed by *Acidithiobacillus thiooxidans*

Hong-rui Chen[1], Duo-rui Zhang[1], Zhen-yuan Nie[1], Jin-lan Xia[1*], Qian Li[1], Rui-yong Zhang[2, 3*], He-hao Yin[1], Eva Pakostova[4]

[1]Key Lab of Biometallurgy of Ministry of Education of China, School of Minerals Processing and Bioengineering, Central South University, Changsha 410083, China

[2]Key Laboratory of Marine Environmental Corrosion and Biofouling, Institute of Oceanology, Chinese Academy of Sciences, Qingdao 266071, China

[3]Open Studio for Marine Corrosion and Protection, Pilot National Laboratory for Marine Science and Technology (Qingdao), Qingdao 266237, China

[4]Centre for Sport, Exercise and Life Sciences, Institute of Health and Wellbeing, Coventry University, Coventry, CV1 5FB, UK

* Correspondence to be addressed: jlxia@csu.edu.cn; ruiyong.zhang@qdio.ac.cn

Abstract

The adsorption of jarosite and the resulting passivation of mineral surfaces can negatively influence metal extraction from sulfidic ores as well as the fate of other elements in biohydrometallurgical processes. Some bioleaching microorganisms mediate dissimilatory iron reduction coupled to sulfur oxidation (DIRSO), a process utilized predominantly in continuously enhanced leaching of metals from sulfide and/or oxidized ores. In this study, the reductive dissolution of jarosite (biosynthesized by the iron-oxidizing archaeon *Acidianus manzaensis*) catalyzed by the mesophilic acidophilic bacterium *Acidithiobacillus* (*At.*) *thiooxidans* oxidizing different inorganic sulfur compounds was investigated. Kinetic measurements of pH, ORP, iron concentrations, and planktonic cell counts were performed to describe the reductive dissolution of jarosite. Moreover, the solid leaching residues were analyzed using X-ray absorption near edge structure (XANES), Inductively coupled plasma - optical emission spectrometry (ICP-OES), scanning electron microscopy (SEM), X-ray diffraction (XRD), and Raman spectroscopy. The dissolution rates of jarosite after 34 days of bioleaching by *At. thiooxidans* with S^0, $Na_2S_2O_3$, and Na_2SO_3 were 41.7, 76.3, and 98.4%, respectively, while negligible jarosite dissolution was detected in abiotic controls. The presence of $Na_2S_2O_3$ and Na_2SO_3 resulted in structural modifications on the jarosite surfaces, but the dissolution of jarosite was not promoted in the absence of *At. thiooxidans*. In the biotic assays with Na_2SO_3, jarosite was completely dissolved, indicating that Na_2SO_3 was the most suitable electron donor (out of those tested) for DIRSO by *At. thiooxidans*. The findings obtained in this study can contribute to designing suitable bioleaching strategies for oxidized ores. They also highlight the potential of microbially catalyzed DIRSO to mitigate jarosite formation that often hinders bioleaching of sulfidic ores.

Key words: *Acidithiobacillus thiooxidans*; jarosite; iron reduction; sulfur oxidation; bioleaching

1. Introduction

Bioleaching is used on an industrial scale for extraction of valuable metals from low-grade sulfide ores and gold concentrates, and similar microbial processes also play an important role in *in situ* remediation of sites contaminated with harmful heavy metals and radioactive elements. Bioleaching is considered the most environmentally friendly metallurgical technology in the 21st century that is economically feasible (Jia et al. 2020; Liao et al. 2020; Schippers et al. 2013). The sulfide ore dissolution mechanism includes thiosulfate and polysulfide pathways (Schippers and Sand 1999). Fe(II) and sulfur exposed on mineral surface or released into solution serve as electron donors for bioleaching bacteria and archaea, while Fe^{3+} and acidity (in the form of H^{+}) respectively are produced in the oxidation processes catalyzed by these mineral-oxidizing prokaryotes.

Bioleaching as well as the generation of acid mine drainage (AMD) are driven primarily by aerobic (bio)oxidation of iron and sulfur compounds. Both processes are also greatly influenced by microbial dissimilatory iron reduction coupled to sulfur oxidation (DIRSO), which has been described for anaerobic as well as aerobic conditions at very low pH $\leq$ 2 (Marrero et al. 2015; Osorio et al. 2013). However, DIRSO has not yet been fully elucidated; particularly iron and sulfur speciation transformations during DIRSO, microbial community structure and function, and the molecular mechanisms of iron and sulfur redox transformations remain to be described and require further research.

Bioleaching and the generation and release of AMD is usually accompanied by the formation of large amounts of secondary iron hydroxysulfate minerals including schwertmannite $Fe_8O_8(OH)_{8-2x}(SO_4)_x$, goethite α-FeOOH, and jarosites $MFe_3(SO_4)_2(OH)_6$ ($M=K^+$, Na^+, NH_4^+, H_3O^+). Formation, transformation and dissolution of these secondary minerals are closely related to iron and sulfur oxidation and iron reduction catalyzed by acidophiles, greatly affecting the adsorption and dissolution of metal ions (Acero et al. 2006; Klein et al. 2013; Wang et al. 2006).

In nature, acidophilic iron-reducing microorganisms are phylogenetically and taxonomically diverse (Porsch et al. 2009). They can be heterotrophic, facultatively

autotrophic, and obligately autotrophic bacteria or archaea that live via chemoheterotrophy (organic matter as electron donor) or chemoautotrophy (H_2 or reduced inorganic sulfur compounds as electron donors) by reducing various Fe^{3+} minerals (e.g., akageneite β-FeOOH, amorphous ferrihydrite $Fe(OH)_3$, goethite α-FeOOH, magnetite Fe_3O_4, jarosites, and schwertmannite) (Bridge and Johnson 2000; Giaveno et al. 2013; Hedrich and Johnson 2013; Johnson 1998; Vargas et al. 1998; Yoshida et al. 2006). There is evidence that the kinetics of dissimilatory reduction of Fe^{3+} compounds is related to their structure as well as the speciation and concentration of the electron donor(s) (Coupland and Johnson 2008). Moreover, the type of the microorganism(s) (including the microbial community structure) and environmental factors (such as oxygen concentration, pH value, redox potential, and others) affect Fe^{3+} reduction rates (Baker and Banfield 2003; Bridge and Johnson 1998; Marrero et al. 2017; Ohmura et al. 2002; Sand 1989).

It has been previously shown that the oxidation of sulfide minerals catalyzed by aerobic prokaryotes involves complex iron and sulfur speciation and phase transformations, in which the iron and sulfur secondary minerals (including jarosites) and sulfur intermediates can strongly affect the bioleaching processes (Johnson et al. 2017; Liu et al. 2016; Schippers et al. 1996; Schippers and Sand 1999; Xia et al. 2010; Yang et al. 2016). The secondary minerals and elemental sulfur (S^0) may accumulate and precipitate on the mineral surfaces, thus forming a passivation layer hindering the bioleaching process (Injae et al. 2018; Klauber et al. 2001; Smith et al. 2006; Vera et al. 2013; Xia et al. 2010; Zhu et al. 2011). Some intermediates (such as S^0, which can occur in a crystalline phase), together with changes in system conditions (such as temperature, sodium chloride concentration, and others), can result in transformation and activity changes in the bioleaching systems (Liang et al. 2012; Ma et al. 2017; Yin et al. 2020; Zhu et al. 2011). Continuous changes in chemical structure and speciation of mineral surfaces during leaching may affect the interactions between microorganisms and mineral surfaces (Yang et al. 2021), which can further inhibit the bioleaching process (Xia et al. 2020; Xiong et al. 2015). An effective removal of jarosites and accumulated

100 S^0 (generated in oxidative bioleaching processes) is a way to improve the
101 microorganism-mineral interaction and enhance the efficiency of oxidative bioleaching
102 of sulfide mineral ores (Norris et al. 2015). So far, there are few studies on iron and
103 sulfur speciation and phase transformation under anaerobic condition.

104 There are at least two archaeal and eight bacterial phyla that catalyze DIRSO for
105 autotrophic growth (Baker and Banfield 2003; Johnson and McGinness 1991; Kucera
106 et al. 2012a; Kucera et al. 2012b). Previous studies mainly concentrated on anaerobic
107 bioleaching processes catalyzed by mesophilic acidophiles (Egger et al. 2016; Eisele
108 and Gabby 2014; Klatt and Polerecky 2015; Marrero et al. 2017) and comparative
109 studies on metabolic pathways of bioleaching microorganisms under anaerobic
110 conditions (Coram and Rawlings 2002; Hedrich and Johnson 2013; Norris et al. 2018;
111 Ohmura et al. 2002; Okibe et al. 2003). It is worth noting that some acidophilic
112 chemolithotrophs respiring by DIRSO can also couple reduction of Fe^{3+} or S^0 with H_2
113 oxidation under anaerobic conditions (Ohmura et al. 2002). Studies on anaerobic
114 respiratory patterns in acidophilic microorganisms are scarce and further research needs
115 to be carried out to describe these processes sufficiently.

116 Till today, the relevance of DIRSO catalyzed by acidophilic microorganisms in
117 bioleaching applications and AMD environments is still unclear, due to the lack of
118 published data. Studies are required e.g., on the mechanism(s) involved in DIRSO
119 under anaerobic (but also aerobic) conditions. In the current study, the capacity of the
120 mesophilic acidophile *At. thiooxidans* to couple sulfur oxidation with Fe^{3+} reduction
121 under anaerobic conditions was investigated, together with the effects of different
122 inorganic sulfur compounds on the reduction of jarosite.

123 **2. Materials and methods**

124 2.1 Bacterial strain of *At. thiooxidans* and culture conditions

125 The bacterial strain *At. thiooxidans* DSM 504 was obtained from the Key
126 Laboratory of Biometallurgy of the Ministry of Education of China (Changsha, China).
127 The strain was grown and maintained in a basal salts medium (pH = 2.0 ± 0.05)
128 containing (in g/L): $(NH_4)_2SO_4$, 3.0; $MgSO_4$, 0.5; K_2HPO_4, 0.5; KCl, 0.1; $Ca(NO_3)_2$,

129 0.01, and supplemented with 10 g/L of S^0 serving as electron donor for *At. thiooxidans*.
130 The culture was cultivated in an incubator (ZHTY-70S, Shanghai Zhichu Instruments,
131 China) at 30 ℃ and 180 rpm.

132 2.2 Preparation of potassium jarosite using *Acidianus (Aa). manzaensis*

133 Potassium jarosite (Pj) was biosynthesized using a pure culture of the extremely
134 thermophilic archaeon *Aa. manzaensis,* which is known for its high Fe^{2+} oxidation
135 activity compared to mesophilic acidophilic bacteria. The Pj synthesis process was
136 carried out in 250 mL Erlenmeyer flasks containing 100 mL basal salts medium
137 (described above; pH 2.0 ± 0.05). A 1.5:1 molar ratio of Fe to K in the Pj synthesis
138 system was achieved by adding 0.2 mol/L $FeSO_4$ and 0.067 mol/L K_2SO_4, prior to the
139 inoculation with *Aa. manzaensis* (to initial concentration of 2×10^8 cells/mL). The
140 flasks were cultivated in a thermostatic shaker at 65 °C and 180 rpm. After all Fe^{2+} in
141 the solution was biooxidized to Fe^{3+} (after approx. 6 days), the precipitate was filtered
142 through a 0.22 μm cellulose nitrate membrane. The obtained precipitate was washed by
143 deoxygenated ultrapure water for several times, and dried in a vacuum oven at 30 ℃.

144 2.3 Sulfur oxidation coupled to Pj dissolution by *At. thiooxidans*

145 Anaerobic Pj dissolution experiments were performed in 150 mL serum bottles,
146 each containing 50 mL sterile basal salts medium (pH 1.94 ± 0.05, adjusted with 1 M
147 H_2SO_4) and 0.5 g Pj. Three inorganic sulfur compounds were selected (at a sulfur
148 concentration equivalent to 10 g/L) to be tested: S^0, $Na_2S_2O_3$, and Na_2SO_3. In biotic
149 assays, the initial cell density of *At. thiooxidans* was 4×10^8 cells/mL, while
150 uninoculated sterile assays served as abiotic controls for each inorganic sulfur
151 compound.

152 Standard anaerobic techniques were used in this study. Sterilized medium (121 °C,
153 30 minutes) was aliquoted into sterile serum bottles. The bottles containing complete
154 assays (described above) were capped with sterilized butyl rubbers stoppers and sealed
155 with aluminum crimps. The assays were then vigorously bubbled for approximately 20
156 min via a filter (0.22 μm) with N_2:CO_2 (80/20, v/v) to remove dissolved oxygen.

All assays were performed in duplicate in a thermostatic shaker at 30 °C and 180 rpm. Liquid samples were taken every 2-4 days, to monitor changes in physicochemical parameters in the solution. Before sampling, the serum bottle stoppers were disinfected with ethanol. Sampling was carried out with sterile syringes, which were prior to use deoxygenated with a mixture of N_2/CO_2 passed via a sterile filter (0.22 μm).

2.4 Analytical methods

Planktonic cell counts were determined under a light microscope (Olympus, CX33, Japan), using a bacterial counting plate (HD-852). The concentration of dissolved total ($[Fe^T]_{aq}$) and ferric ($[Fe^{3+}]_{aq}$) iron was determined by the sulfosalicylic acid method (Karamanev et al. 2002), and the concentration of dissolved ferrous iron ($[Fe^{2+}]_{aq}$) was calculated by subtracting $[Fe^{3+}]$ from $[Fe^T]$. The concentration of other metal elements was determined using an inductively coupled plasma-optical emission spectrometer (ICP-OES; SPECTRO BLUE SOP, Spike Analytical Instruments, Germany). The pH value and redox potential (ORP) were monitored using a pH meter (PB-10, Beijing Sartorius Scientific Instrument Co. Ltd., China) and potentiometer (PHSJ-4F, Shanghai Inesa Scientific Instruments Co. Ltd., China).

The morphological features of solid samples were characterized by scanning electron microscopy (SEM; TESCA MIRA4, Czech Republic). The phase and chemical compositions were analyzed using an X-ray diffractometer (XRD; D8 Advance, Bruker, Germany) and a laser Raman spectrometer (Jobin Yvon LabRam-010, France). Sulfur and iron speciation in solid residues were characterized by S K-edge and Fe L-edge X-ray absorption near edge structure (XANES) spectroscopy at beamlines 4B9A and 4B7B, respectively, at Beijing Synchrotron Radiation Facility (BSRF), Beijing, China.

3 Results and discussion

3.1 Characterization of biosynthesized Pj

Oxidation of Fe^{2+} (Equation 1) catalyzed by *Aa. manzensis* mediated the formation of Pj. After 6 days of microbial oxidation, there was no residual Fe^{2+} detected in the solution and $[Fe^T]$ and $[Fe^{3+}]$ were significantly lowered. The synthesized iron-rich

precipitate was of an ochre yellow color (Supplementary Figure S1). The results of ICP-OES analysis (Table 1) showed that the contents of Fe, K, and S in the biosynthetic Pj were 31.2, 5.3, and 12.1%, respectively. The molar ratio of Fe/S was 1.48:1, which was very close to the theoretical value of standard Pj (Drouet and Navrotsky 2002). This indicated a high purity of the Pj synthesized by the oxidation activity of *Aa. manzensis*.

$$4Fe^{2+} + 4H^{+} + O_2 \xrightarrow{\text{Microbial}} 4Fe^{3+} + 2H_2O \quad (1)$$

Table 1. Summary of chemical composition of Pj biosynthesized by *Aa. manzensis,* compared to that of standard Pj.

	Fe (%)	K (%)	S (%)	Fe/S molar ratio
Biosynthesized Pj	31.23	5.33	12.11	1.48:1
Standard Pj*	33.45	7.78	12.81	1.50:1

The biosynthesized Pj was crystallized, showing a fine rhomboid structure with glass luster. The particle size was approximately 25 μm (Figure 1a, b). The results of an XRD analysis (Fig. 1c) showed the presence of a diffraction peak in the biosynthesized Pj identical to that of a standard Pj (PDF #71-1777), confirming the high purity of the biosynthesized Pj.

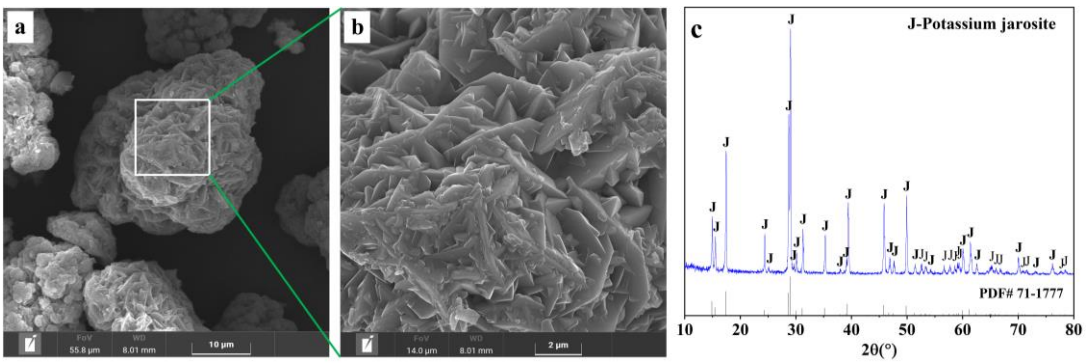

Figure 1. (a, b) SEM images and (c) XRD pattern of the biosynthesized Pj.

3.2 Reductive dissolution of Pj by different inorganic sulfur compounds oxidized by At. thiooxidans

The dissolution of Pj over time, as a result of Fe^{3+} reduction coupled to sulfur oxidation (Equation 2) catalyzed by *At. thiooxidans*, is shown in Figure 2, with soluble $[Fe^{T}]_{aq}$ and $[Fe^{2+}]_{aq}$ reflecting the Fe^{3+} reducing ability of the bacterium.

$$S^0 + 6Fe^{3+} + 4H_2O \xrightarrow{At.\ thiooxidans} 6Fe^{2+} + SO_4{}^{2-} + 8H^+ \quad (2)$$

The bioleaching assays with Na_2SO_3 as electron donor showed greater $[Fe^T]_{aq}$ compared to the other biotic assays (Figure 2a). In the bioleaching assays with S^0 and $Na_2S_2O_3$, $[Fe^T]_{aq}$ changed only marginally in the first 10 days, after which it gradually increased. The efficiency of Pj dissolution was higher using $Na_2S_2O_3$ than that with S^0. It can be seen that the iron ions released into solution following the dissolution of Pj were rapidly reduced to Fe^{2+} (Figure 2b), indicating that *At. thiooxidans* DSM 504 has the capability of performing DIRSO under anaerobic conditions. Importantly, the results showed that the sulfur source type may directly affect Fe^{3+} reduction and thus the efficiency of jarosite dissolution.

In the assays with Na_2SO_3, $[Fe^{2+}]$ decreased from day 15 to 17, and also from day 30 to 34. XANES analysis (Figure 8) confirmed the presence of Fe^{2+} in the solid precipitates, likely as ferrous sulfate (which can be formed by the reaction of excessive sulfate from Pj dissolution with Fe^{2+}).

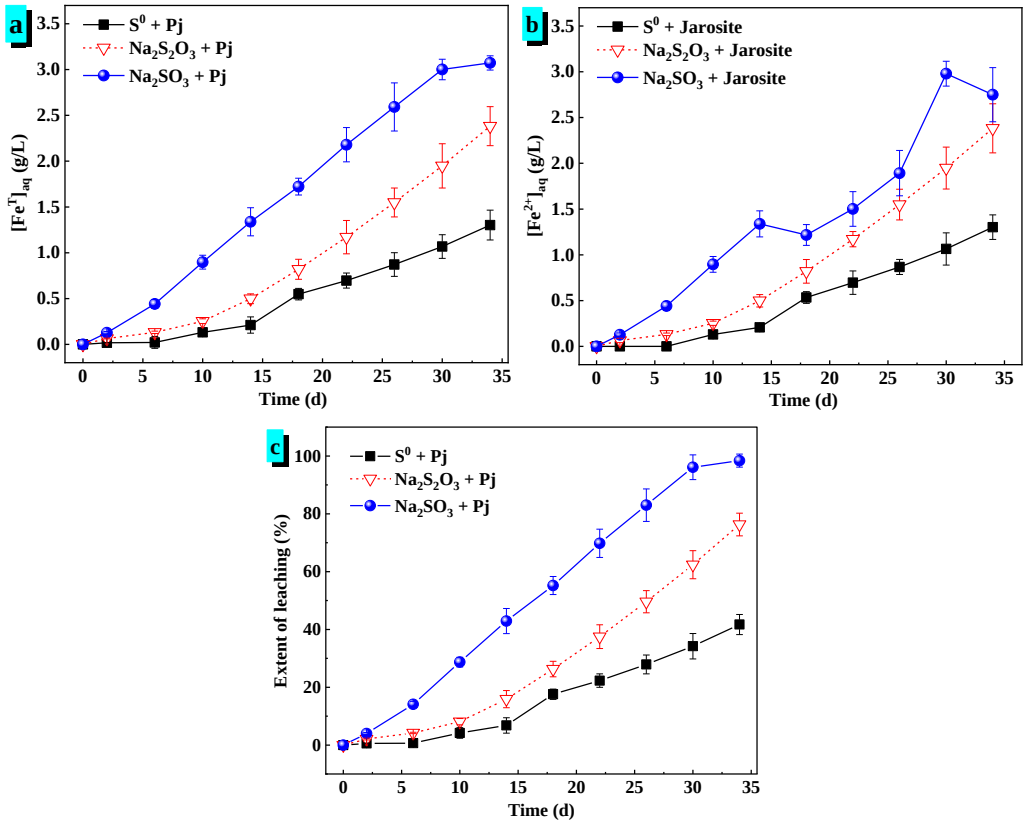

Figure 2. Changes in (a) $[Fe^T]_{aq}$ and (b) $[Fe^{2+}]_{aq}$ during Pj bioleaching, and (c) the extent of leaching of Pj by different inorganic sulfur compounds (S^0, $Na_2S_2O_3$, and Na_2SO_3)

223 catalyzed by *At. thiooxidans*.

224 Figures 2c shows the extent of leaching of Pj using S^0, $Na_2S_2O_3$, and Na_2SO_3 as
225 inorganic sulfur compounds catalyzed by *At. thiooxidans*. In the first 6 days, the
226 leaching rates in the assays with S^0 and $Na_2S_2O_3$ reached only 0.7 and 4.2%, which were
227 significantly lower values than that of the assay with Na_2SO_3 (14.1%).

228 Oxidation of S^0 by acidophilic sulfur-oxidizing prokaryotes is a complex process
229 that involves the attachment of cells to sulfur particles and transportation of sulfur into
230 the cells for further oxidation, with the formation of extracellular polymeric substances
231 (EPS) being a prerequisite for the initial attachment of bacterial cells to hydrophobic
232 sulfur particles (Rohwerder and Sand 2007; Zhang et al. 2008; Zhang et al. 2019). That
233 is why anaerobic oxidation of S^0 may be slow compared to anaerobic oxidation of
234 soluble sulfur compounds. Indeed, S^0 often accumulates as the main component of
235 passivation layers formed during bioleaching on the surfaces of sulfide minerals (such
236 as arsenopyrite and chalcopyrite), thus lowering the efficiency of the leaching processes
237 (Klauber 2008; Klauber et al. 2001).

238 Thiosulfate ($S_2O_3^{2-}$) is one of the common intermediate products in sulfide mineral
239 bioleaching processes (Schippers and Sand 1999). Under acidic conditions, $S_2O_3^{2-}$ often
240 reacts with H^+ to form $H_2S_2O_3$ (Equation 3), which is then quickly converted to S^0
241 (Equation 4). This process significantly reduces the efficiency of microbial sulfur
242 oxidation, resulting in low Pj dissolution in early leaching periods (as shown in Figure
243 2c). In this study, the dissolution of Pj in the assays with S^0, $Na_2S_2O_3$, and Na_2SO_3
244 began to rapidly increase after 6 days of bioleaching (with the following order of
245 increasing leaching rates: $S^0 < Na_2S_2O_3 < Na_2SO_3$. After 34 days, the final leaching of
246 Pj in the above three assays reached 41.7, 76.3, and 96.4%, respectively (Figure 2c).
247 The dissolved iron was mainly in the form of Fe^{2+} (Figures 2a, b). For the abiotic
248 controls, the maximum leaching rate of Pj in the assay with S^0, $Na_2S_2O_3$, and Na_2SO_3
249 reached only 1.5, 6.3, and 8.7%, respectively (Supplementary Figure S2), and dissolved
250 iron of all these abiotic assays was present in the form of Fe^{2+} (Supplementary Figure
251 S3). The above results clearly indicate that *At. thiooxidans* DSM 504 can use inorganic

sulfur compounds as an electron donor to promote the reduction of Fe^{3+} under anaerobic conditions (Ohmura et al. 2002). Cells of *At. thiooxidans* DSM 504 play a key role in the Pj dissolution process, although Na_2SO_3 and $Na_2S_2O_3$ can reduce a small amount of Fe(III) to Fe(II) in the early stage (Supplementary Figure S3b).

$$S_2O_3{}^{2-} + 2H^+ \rightarrow H_2S_2O_3 \quad (3)$$

$$H_2S_2O_3 \rightarrow SO_2(g) + S(s) + H_2O \quad (4)$$

The changes in pH, ORP, and cell density in solution during the anaerobic reduction of Pj by *At. thiooxidans* are shown in Figure 3. The pH in the assay with S^0 gradually decreased to about 1.6 in the first 14 days, influenced predominantly by bacterial S^0 oxidation (which is a H^+-generating process; Equation 2) and by Pj dissolution (H^+-consuming process; Equation 5). Due to slow dissolution of Pj in the early stages (Figure 3c), the bio-oxidation of S^0 was the primary factor affecting the pH, resulting in a net pH decrease. After 14 days, the pH began to increase slowly as the rate of Pj dissolution accelerated. In the assays with Na_2SO_3, the pH in the solution dropped rapidly in the first 6 days, likely due to the quick bio-oxidation of $SO_3{}^{2-}$ (Equation 6) catalyzed by *At. thiooxidans*, which is significantly faster than that of other inorganic sulfur compounds.

$$KFe_3(SO_4)_2(OH)_6 + 6H^+ \leftrightharpoons K^+ + 3Fe^{3+} + 2SO_4{}^{2-} + 6H_2O \quad (5)$$

$$SO_3{}^{2-} + 2Fe^{3+} + H_2O \rightarrow 2Fe^{2+} + SO_4{}^{2-} + 2H^+ \quad (6)$$

In the assays with $Na_2S_2O_3$, the H^+-consuming reaction (Equation 3) leading to $S_2O_3{}^{2-}$ disproportionation (Equation 4) caused the rapid increase in pH in the early leaching stage (pH reached the maximum value of 2.85 on day 10). Generally, the pH in the assays with $S_2O_3{}^{2-}$ was significantly higher than pH in other assays, throughout the whole course of the experiment (Figure 3a). Despite such pH values (> 2.5) being above the growth optimum of *At. thiooxidans*, the Pj dissolution rate was not significantly inhibited (as shown in Figure 2c). In addition, the gradual accumulation of Fe^{2+} in the later stage of the leaching process resulted in a significant decrease in ORP values (that are determined by $[Fe^{3+}]/[Fe^{2+}]$ and indirectly by decreasing $[H^+]$ due to the $S_2O_3{}^{2-}$ degradation reactions) (Figure 3b). Compared to S^0 and $S_2O_3{}^{2-}$, $SO_3{}^{2-}$ was

more easily and quickly utilized by *At. thiooxidans* as an electron donor under anaerobic conditions. Although the planktonic cell counts did not significantly increase in the assay with SO_3^{2-} (Figure 3c), the efficiency of Fe^{3+} reduction and Pj dissolution was relatively high.

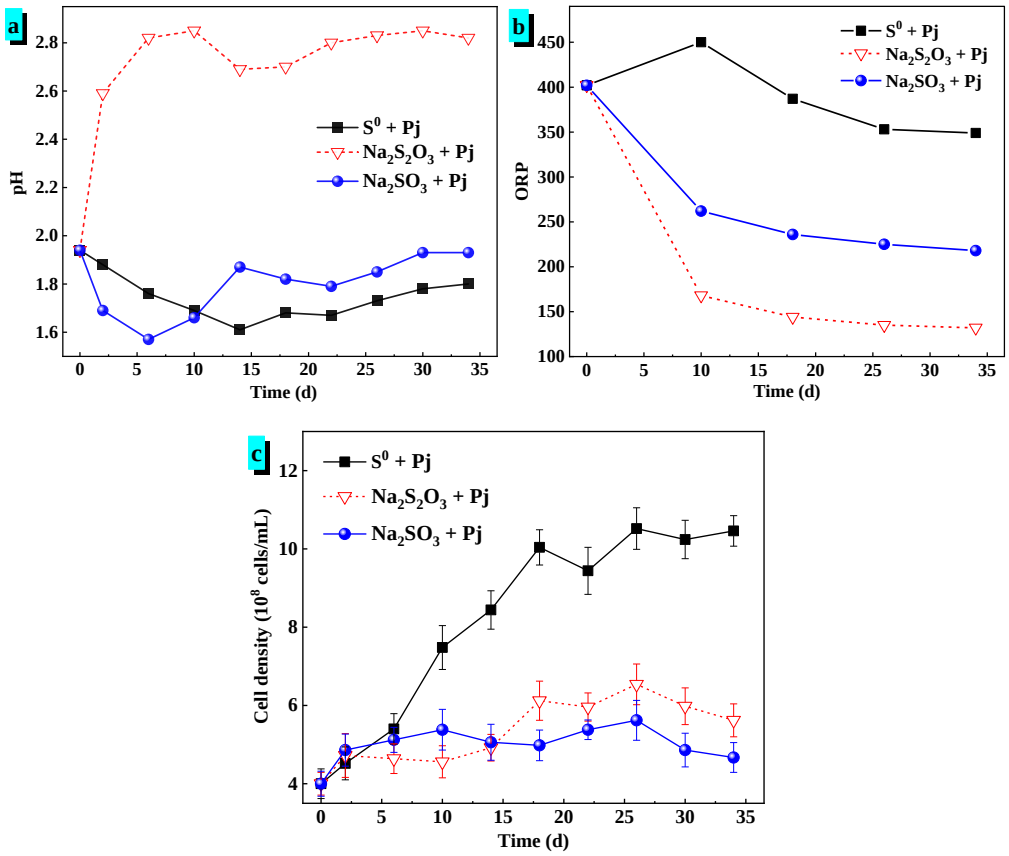

Figure 3. Changes in (a) pH, (b) ORP, and (c) planktonic cell counts during anaerobic reduction of Pj by different inorganic sulfur compounds (S^0, $Na_2S_2O_3$, and Na_2SO_3) catalyzed by *At. thiooxidans*.

For the abiotic controls (containing S^0, $Na_2S_2O_3$, and Na_2SO_3), both the pH and ORP values had no significant changes throughout the process (Figure S4), indicating no apparent dissolution of Pj and redox reaction of iron or sulfur occurred.

The above findings show that the type of a sulfur source can significantly affect pH and ORP values during reductive bioleaching, as well as the Fe^{3+} reduction and jarosite dissolution rates. Therefore, it is particularly important to consider the suitability of a selected sulfur source when designing strategies for industrial applications of reductive bioleaching of oxidized ores.

298 *3.3 Characterization of solid leach residues*

299 Large amounts of solid residues were observed at the bottom of the serum bottles
300 after 22 days of reductive bioleaching of Pj and the colors of the assays with the four
301 different inorganic sulfur compounds significantly differed (Figure 4a). In the assays
302 with SO_3^{2-}, the residue turned light yellow, indicating the Pj was partially dissolved.
303 The colors of the solids from the assays with S^0 and $S_2O_3^{2-}$ were visibly darker yellow
304 than the color of the SO_3^{2-} assay residue.

305 After 34 days of Pj bioleaching, the assays with SO_3^{2-} turned clear and the Pj
306 completely dissolved. The color of the solid residues in the assays with S^0 and $S_2O_3^{2-}$
307 was also significantly lighter compared to the colors on day 22 (Figure 4b). It is worth
308 noting that the final color of the residues in the assays with $S_2O_3^{2-}$ resembled that of
309 colloidal sulfur, indicating the accumulation of S^0. No significant color changes were
310 observed in abiotic controls after 34 days of incubation (Figure 4c), which strongly
311 indicated the importance of microbial activity in Pj dissolution under anaerobic
312 conditions.

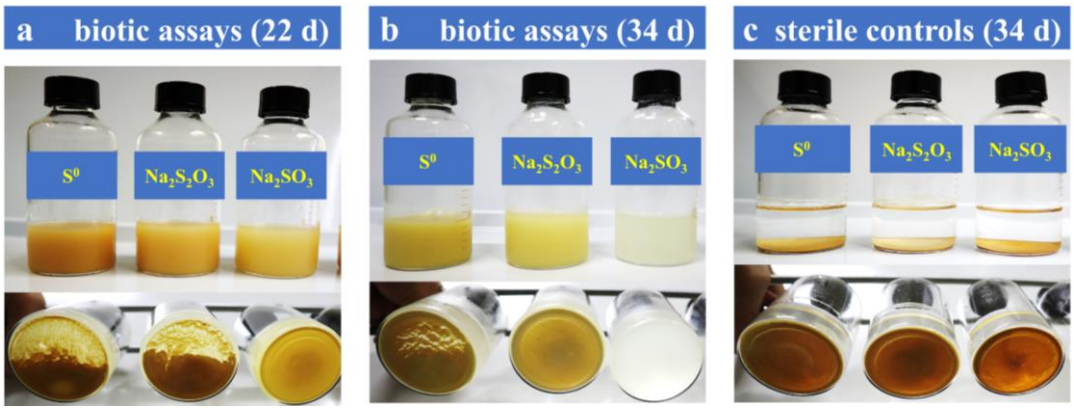

313

314 **Figure 4.** Colors of the solutions and leach residues during anaerobic reduction of Pj
315 by different inorganic sulfur compounds catalyzed by *At. thiooxidans* after (a) 22 and
316 (b) 34 days, and (c) those of the sterile controls after 34 days.

317 To compare the surface structure of Pj leach residues, the solids from both
318 bioleaching assays and abiotic controls were collected after 34 days and characterized
319 by SEM (Figure 5). The solid phase from the assays with S^0 (Figure 5a) was dominated
320 by the characteristic morphologies of S^0 and Pj. The surface of S^0 was visibly corroded

by *At. thiooxidans* cells. Although the surface of the Pj particles was also modified, there were still particles of a size > 10 μm detected. In the assays with $S_2O_3^{2-}$ (Figure 5b), the leach residues were characterized as smooth particles with a size < 5 μm. In the assays with SO_3^{2-} (Figure 5c), the fine particle-sized residues were poorly crystallized and the morphological characteristics of Pj were not detected.

In the abiotic assays with S^0 (Figure 5d), smooth and flat surfaces were identified as S^0, while Pj was identified as large particles with distinct edges and crystals. The surface morphology of Pj was modified from flat and even to poorly crystallized fragments in residues from the abiotic assays with $S_2O_3^{2-}$ (Figure 5e) and particularly from those with SO_3^{2-} (Figure 5f). It is possible that such abiotic modifications in microstructures on Pj surfaces may help accelerate DIRSO by acidophilic prokaryotes (such as *At. thiooxidans* and others).

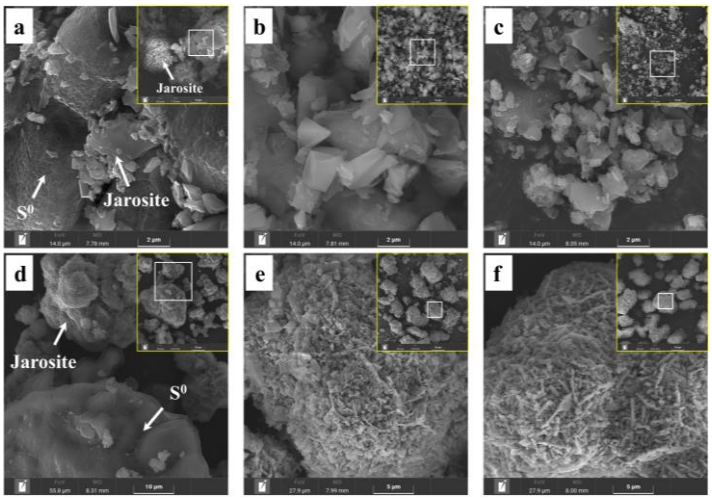

Figure 5. SEM images of Pj leaching residues in the bioleaching assays with different inorganic sulfur compounds: (a) S^0, (b) $Na_2S_2O_3$, and (c) Na_2SO_3, as well as in sterile controls with (d) S^0, (e) $Na_2S_2O_3$, and (f) Na_2SO_3. All solid residues were collected after 34 days of incubation.

Raman spectroscopy serves as a powerful tool in the identification of sulfur speciation, and the technique was used in this study to further characterize the leaching residues. As marked in Figure 6a, the biosynthesized Pj had significant feature peaks at 138, 223, 433, 1006, and 1103 cm^{-1}. The leach residues collected from the assays with

S^0 showed significantly lower intensity of the peaks corresponding to Pj, compared to residues from the abiotic assays. In the assays with $S_2O_3^{2-}$, residues showed peaks corresponding to S^0 (at 152, 217, and 472 cm^{-1}) in addition to those corresponding to Pj (Figure 6b). This indicates that $S_2O_3^{2-}$ was partially converted to S^0, confirming the observations by SEM (shown in Figure 5b). This partial conversion might be a reason for a slower Pj dissolution in the assays with $S_2O_3^{2-}$ compared to that in the assays with SO_3^{2-}. The peaks characteristic for Pj were not detected in the residues from the assays with SO_3^{2-}. No significant changes were detected in the peaks of the residue from the respective control assays (Figure 6c). In general, the results of the Raman analysis agreed with the color observations (in Figure 4) and SEM data (in Figure 5).

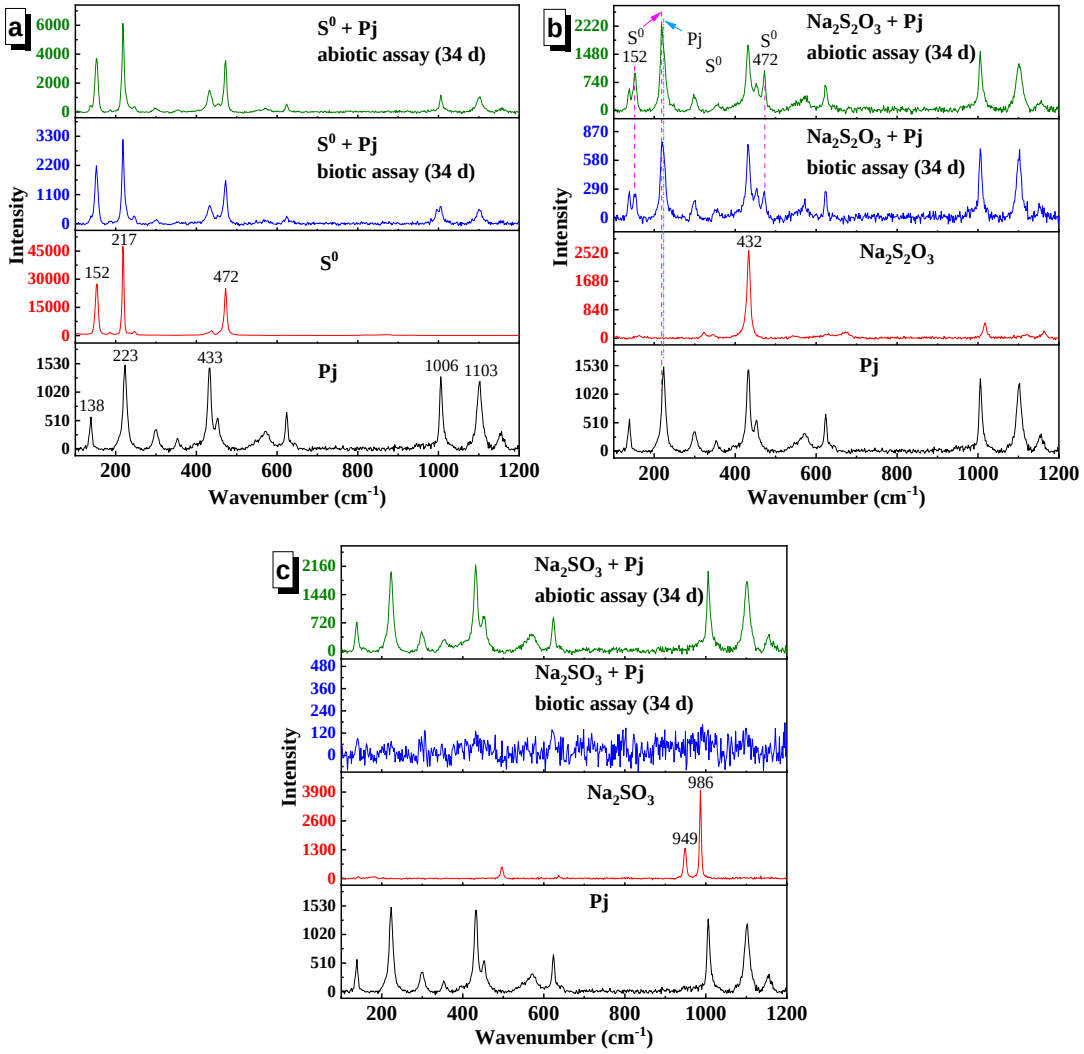

Figure 6. Raman spectra of the residues after abiotic leaching (green lines) and bioleaching by *At. thiooxidans* (blue lines) with (a) S^0, (b) $Na_2S_2O_3$, and (c) Na_2SO_3

after 34 days, compared to Raman spectra of the inorganic sulfur compounds (red lines) and standard Pj specimens (black lines).

Based on the above findings, it can be inferred that Na_2SO_3 was the most suitable electron donor among the tested inorganic sulfur compounds for the reductive dissolution of jarosite, catalyzed by *At. thiooxidans* under the selected conditions. To determine Fe speciation, Fe L-edge XANES analyses of the leached solid residues from both biotic and abiotic assays with Na_2SO_3 were performed. As shown in Figure 7, the initial biosynthesized Pj had two distinct peaks at 708.5 and 722.1 eV corresponding to Fe^{3+}, while $FeSO_4$ had two peaks at 706.8 and 720.1 eV corresponding to Fe^{2+}. A comparison of the spectra indicated that the Fe species in the final bioleaching residues were $FeSO_4$. No peaks corresponding to jarosite and Fe^{3+} were detected (Figure 7), confirming the complete disappearance of the jarosite (as previously determined by SEM and the visible changes in assay color). In contrast, no peaks corresponding to Fe^{2+} were detected in the leached residues from the abiotic controls, and all detected peaks in these assays were identified as jarosite. The results show that Na_2SO_3 alone could not mediate Pj dissolution under anaerobic conditions, indicating that *At. thiooxidans* cells played a key role in Pj dissolution. The dissolution of jarosites has vast implications for industrial bioleaching, especially reductive bioleaching of oxidized ores (Johnson et al. 2013), but also for Fe^{2+} oxidation-based processes.

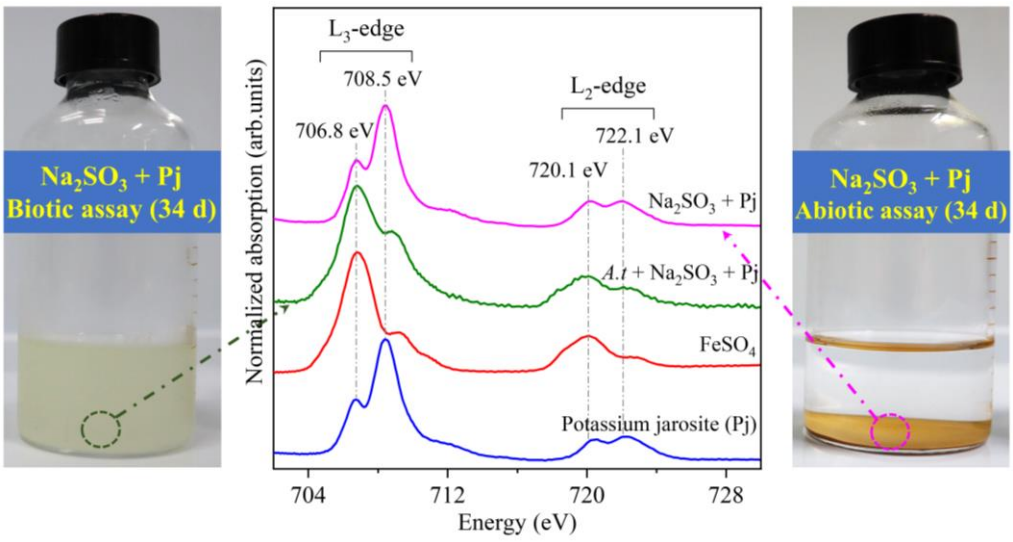

Figure 7. Fe L-edge XANES spectra of the solid residues collected from the biotic and

abiotic assays with Na_2SO_3 (after 34 days of Pj leaching), compared to the spectra of Fe-bearing standards (biosynthesized Pj and $FeSO_4$).

Sulfur speciation is another important parameter describing the composition of solid residues from leaching processes. The S K-edge XANES analysis was used to determine the sulfur speciation in the Pj leach residues collected in this study (Figure 8). The S K-edge XANES spectra of different sulfur standards showed significant variations in the position, intensity, and shape of the peaks (Figure 8a). The spectra of sulfur standards, i.e., S^0, Na_2SO_3, Na_2SO_4, and jarosite were characterized by peaks at 2472.4, 2478.2, 2482.6, and 2482.8 eV, respectively, while the spectrum of $Na_2S_2O_3$ had two peaks at 2471.8 and 2480.8 eV. Figure 8b shows the S K-edge XANES spectrum of the Pj bioleaching residues. A comparison with the spectra of sulfur standards revealed the presence of residual S^0 in the solids from the assays with S^0 and the main peak at 2482.8 eV indicated the presence of undissolved jarosite. In the assays with SO_3^{2-}, the main peak at 2482.6 eV corresponded to the characteristic peak of Na_2SO_4, indicating that SO_3^{2-} was rapidly oxidized to SO_4^{2-} under anaerobic conditions. The electrons from SO_3^{2-} were used to reduce the Fe^{3+} in the jarosite, causing its rapid dissolution. In the assays with $S_2O_3^{2-}$, the residues showed a strong absorption peak at 2472.4 eV, supporting the previous hypothesis indicating that a portion of the $S_2O_3^{2-}$ was converted into S^0, which would explain the relatively slow dissolution of jarosite in these assays.

For all residues from the sterile controls, the position of the main peak was at 2482.8 eV (Figure 8c), confirming limited dissolution of jarosite in the abiotic systems. In both biotic and abiotic assays with $S_2O_3^{2-}$, the residue spectra showed a peak at 2472.4 eV (characteristic for S^0), indicating that conversion of $S_2O_3^{2-}$ to S^0 occurred both in the presence and absence of microorganisms (Schippers and Sand 1999).

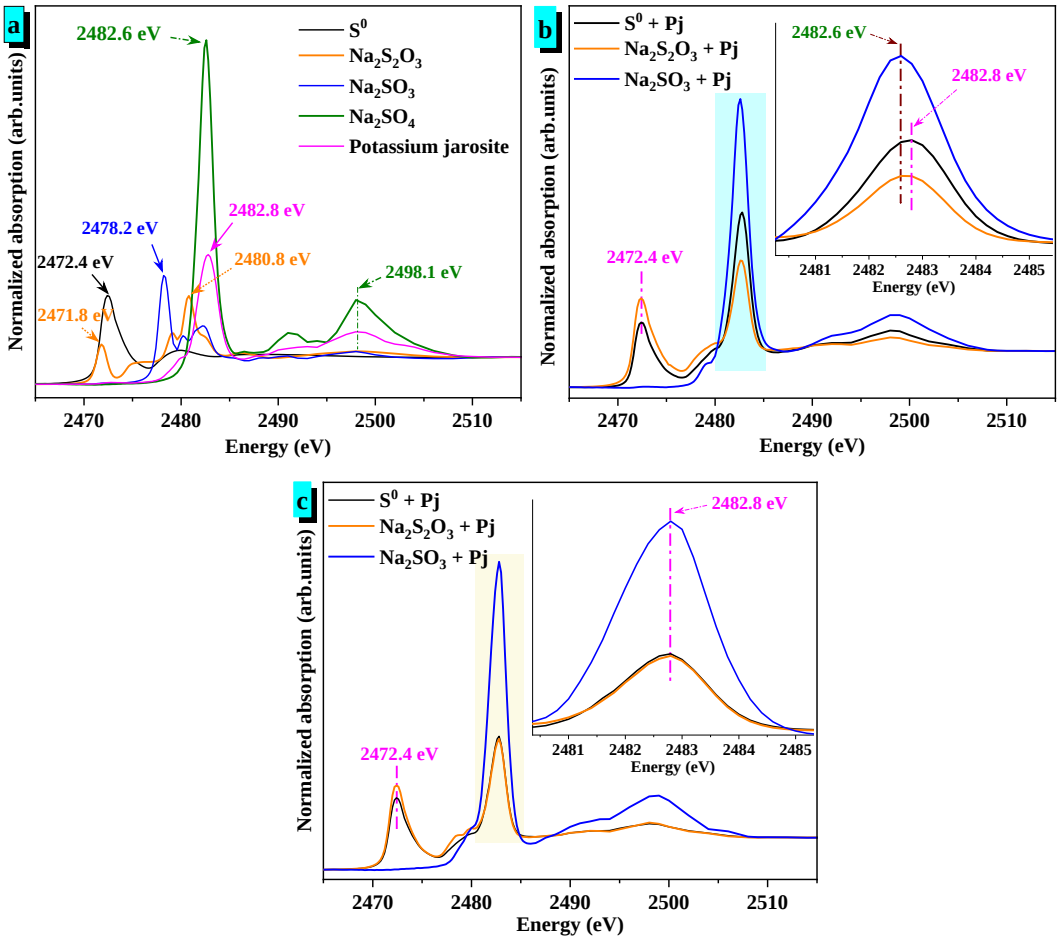

Figure 8. S K-edge XANES spectra of (a) S-bearing standards (S^0, $Na_2S_2O_3$, Na_2SO_3, Na_2SO_4, and Pj), and the Pj residues collected on day 34 from the (b) biotic and (c) abiotic Pj leaching systems with different inorganic sulfur compounds.

4 Conclusions

The influence of three inorganic sulfur compounds on dissimilatory Fe^{3+} reduction catalyzed by an acidophilic sulfur-oxidizing bacterium was investigated. The dissolution of microbially synthesized jarosite catalyzed by *At. thiooxidans* was conducted at anaerobic conditions, yielding the dissolution rates of 41.7, 76.3, and 98.4% after 34 days of bioleaching with S^0, $Na_2S_2O_3$, and Na_2SO_3, respectively. The findings primarily highlight the importance of the use of a suitable sulfur source, particularly in DIRSO-based bioleaching applications, to mitigate jarosite formation negatively impacting the efficacy of bioleaching processes. Given the importance of jarosite minerals in hydrometallurgical applications as well as in acidic and mining environments (Cogram 2018), it is crucial to design suitable strategies for reductive bioleaching that utilize DIRSO.

Acknowledgements

This work was supported by the National Natural Science Foundation of China (Nos. 51861135305, 42076044), the financial support from the National Key Research and Development Program of China (2018YFE0110200), and the Open Funds of Beijing Synchrotron Radiation Facility (2020-BEPC-PT-003789, 2020-BEPC-ZD-000184).

References

Acero, P., Ayora, C., Torrentó, C., Nieto, J.-M., 2006. The behavior of trace elements during schwertmannite precipitation and subsequent transformation into goethite and jarosite. Geochim. Cosmochim. Acta, 70(16): 4130-4139.

Baker, B.J., Banfield, J.F., 2003. Microbial communities in acid mine drainage. FEMS Microbiol. Ecol., 44(2): 139-152.

Bridge, T.A., Johnson, D.B., 1998. Reduction of soluble iron and reductive dissolution of ferric iron-containing minerals by moderately thermophilic iron-oxidizing bacteria. Appl. Environ. Microbiol., 64(6): 2181-2186.

Bridge, T.A., Johnson, D.B., 2000. Reductive dissolution of ferric iron minerals by *Acidiphilium* SJH. Geomicrobiol. J., 17(3): 193-206.

Cogram, P., 2018. Jarosite. In: Earth Systems and Environmental Sciences, Elsevier, pp. 1-9.

Coram, N.J., Rawlings, D.E., 2002. Molecular relationship between two groups of the genus *Leptospirillum* and the finding that *Leptospirillum ferriphilum* sp. nov. dominates South African commercial biooxidation tanks that operate at 40 C. Appl. Environ. Microbiol., 68(2): 838-845.

Coupland, K., Johnson, D.B., 2008. Evidence that the potential for dissimilatory ferric iron reduction is widespread among acidophilic heterotrophic bacteria. FEMS Microbiol. Lett., 279(1): 30-35.

Drouet, C., Navrotsky, A., 2002. Synthesis, characterization and thermochemistry of K-Na-H_3O Jarosites. Geochim. Cosmochim. Acta, 67(11): 2063-2076.

Egger, M., Kraal, P., Jilbert, T., Sulu-Gambari, F., Sapart, C.J., Röckmann, T., Slomp, C.P., 2016. Anaerobic oxidation of methane alters sediment records of sulfur, iron and phosphorus in the Black Sea. Biogeosciences, 13(18): 5333-5355.

Eisele, T., Gabby, K., 2014. Review of reductive leaching of iron by anaerobic bacteria. Miner. Process. Extr. Metall. Rev., 35(2): 75-105.

Giaveno, M.A., Urbieta, M.S., Ulloa, J.R., Toril, E.G., Donati, E.R., 2013. Physiologic versatility and growth flexibility as the main characteristics of a novel thermoacidophilic *Acidianus* strain isolated from Copahue geothermal area in Argentina. Microb. Ecol., 65(2): 336-346.

Hedrich, S., Johnson, D.B., 2013. Aerobic and anaerobic oxidation of hydrogen by acidophilic bacteria. FEMS Microbiol. Lett., 349(1): 40-45.

Injae, Y., Seungjin, C., and Jayhyun, P., 2018. Passivation of chalcopyrite in hydrodynamic-bioleaching. EPISODES, 41(4): 249-258.

Jia, L.-P., Huang, J.-J., Ma, Z.-L., Liu, X.-H., Chen, X.-Y., Li, J.-T., He, L.-H., Zhao, Z.-W., 2020. Research and development trends of hydrometallurgy: An overview based on Hydrometallurgy literature from 1975 to 2019. T. Nonferr. Metal. Soc., 30(11): 3147-3160.

Johnson, D.B., 1998. Biodiversity and ecology of acidophilic microorganisms. FEMS Microbiol. Ecol., 27(4): 307-317.

Johnson, D.B., Grail, B.M., Hallberg, K.B., 2013. A new direction for biomining: extraction of metals

462 by reductive dissolution of oxidized ores. Minerals, 3(1): 49-58.
463 Johnson, D.B., Hedrich, S., Pakostova, E., 2017. Indirect redox transformations of iron, copper, and
464 chromium catalyzed by extremely acidophilic bacteria. Front. Microbiol., 8: 211.
465 Johnson, D.B., McGinness, S., 1991. Ferric iron reduction by acidophilic heterotrophic bacteria. Appl.
466 Environ. Microbiol., 57(1): 207-11.
467 Karamanev, D.G., Nikolov, L.N., Mamatarkova, V., 2002. Rapid simultaneous quantitative determination
468 of ferric and ferrous ions in drainage waters and similar solutions. Miner. Eng., 15(5): 341-346.
469 Klatt, J.M., Polerecky, L., 2015. Assessment of the stoichiometry and efficiency of CO_2 fixation coupled
470 to reduced sulfur oxidation. Front. Microbiol., 6: 484.
471 Klauber, C., 2008. A critical review of the surface chemistry of acidic ferric sulphate dissolution of
472 chalcopyrite with regards to hindered dissolution. Int. J. Miner. Process., 86(1): 1-17.
473 Klauber, C., Parker, A., van Bronswijk, W., Watling, H., 2001. Sulphur speciation of leached chalcopyrite
474 surfaces as determined by X-ray photoelectron spectroscopy. Int. J. Miner. Process., 62(1): 65-
475 94.
476 Klein, R., Tischler, J.S., Mühling, M., Schlömann, M., 2013. Bioremediation of mine water. In:
477 Geobiotechnology I. Advances in Biochemical Engineering/Biotechnology. A. Schippers, F.
478 Glombitza and W. Sand (Eds.), Springer-Verlag, Berlin Heidelberg, pp. 109-172.
479 Kucera, J., Bouchal, P., Cerna, H., Potesil, D., Janiczek, O., Zdrahal, Z., Mandl, M., 2012a. Kinetics of
480 anaerobic elemental sulfur oxidation by ferric iron in *Acidithiobacillus ferrooxidans* and protein
481 identification by comparative 2-DE-MS/MS. Antonie Van Leeuwenhoek, 101(3): 561-573.
482 Kucera, J., Zeman, J., Mandl, M., Cerna, H., 2012b. Stoichiometry of bacterial anaerobic oxidation of
483 elemental sulfur by ferric iron. Antonie Van Leeuwenhoek, 101(4): 919-922.
484 Liang, C.-L., Xia, J.-L., Nie, Z.-Y., Yang, Y., Ma, C.-Y., 2012. Effect of sodium chloride on sulfur
485 speciation of chalcopyrite bioleached by the extreme thermophile *Acidianus manzaensis*.
486 Bioresour. Technol., 110: 462-467.
487 Liao, R., Yu, S.-C., Wu, B.-Q., Zhao, C.-X., Lin, H., Hong, M.-X., Wu, H.-Y., Yang, C.-R., Zhang, Y.-S.,
488 Xie, J.-P., 2020. Sulfide mineral bioleaching: Understanding of microbe-chemistry assisted
489 hydrometallurgy technology and acid mine drainage environment protection. J. Cent. South
490 Univ., 27(5): 1367-1372.
491 Liu, X., Chen, B., Chen, J., Zhang, M., Wen, J., Wang, D., Ruan, R., 2016. Spatial variation of microbial
492 community structure in the Zijinshan commercial copper heap bioleaching plant. Miner. Eng.,
493 94: 76-82.
494 Ma, Y.-L., Liu, H.-C., Xia, J.-L., Nie, Z.-Y., Zhu, H.-R., Zhao, Y.-D., Ma, C.-Y., Zheng, L., Hong, C.-H.,
495 Wen, W., 2017. Relatedness between catalytic effect of activated carbon and passivation
496 phenomenon during chalcopyrite bioleaching by mixed thermophilic Archaea culture at 65 °C.
497 T. Nonferr. Metal. Soc., 27(6): 1374-1384.
498 Marrero, J., Coto, O., Goldmann, S., Graupner, T., Schippers, A., 2015. Recovery of nickel and cobalt
499 from laterite tailings by reductive dissolution under aerobic conditions using *Acidithiobacillus*
500 species. Environ. Sci. Technol., 49(11): 6674-6682.
501 Marrero, J., Coto, O., Schippers, A., 2017. Anaerobic and aerobic reductive dissolutions of iron-rich
502 nickel laterite overburden by *Acidithiobacillus*. Hydrometallurgy, 168: 49-55.
503 Norris, P.R., Gould, O.J.P., Ogden, T.J., 2015. Iron solubilization during anaerobic growth of acidophilic
504 microorganisms with a polymetallic sulfide ore. Miner. Eng., 75: 77-84.
505 Norris, P.R., Laigle, L., Slade, S., 2018. Cytochromes in anaerobic growth of *Acidithiobacillus*

*ferrooxidan*s. Microbiology, 164(3): 383-394.

Ohmura, N., Sasaki, K., Matsumoto, N., Saiki, H., 2002. Anaerobic respiration using Fe^{3+}, S^0, and H_2 in the chemolithoautotrophic bacterium *Acidithiobacillus ferrooxidans*. J. Bacteriol., 184(8): 2081-2087.

Okibe, N., Gericke, M., Hallberg, K.B., Johnson, D.B., 2003. Enumeration and characterization of acidophilic microorganisms isolated from a pilot plant stirred-tank bioleaching operation. Appl. Environ. Microbiol., 69(4): 1936-1943.

Osorio, H., Mangold, S., Denis, Y., Ñancucheo, I., Esparza, M., Johnson, D.B., Bonnefoy, V., Dopson, M., Holmes, D.S., 2013. Anaerobic sulfur metabolism coupled to dissimilatory iron reduction in the extremophile *Acidithiobacillus ferrooxidans*. Appl. Environ. Microbiol., 79(7): 2172-2181.

Porsch, K., Meier, J., Kleinsteuber, S., Wendt-Potthoff, K., 2009. Importance of different physiological groups of iron reducing microorganisms in an acidic mining lake remediation experiment. Microb. Ecol., 57(4): 701-17.

Rohwerder, T., Sand, W., 2007. Oxidation of inorganic sulfur compounds in acidophilic prokaryotes. Eng. Life Sci., 7(4): 301-309.

Sand, W., 1989. Ferric iron reduction by *Thiobacillus ferrooxidans* at extremely low pH-values. Biogeochemistry, 7(3): 195-201.

Schippers, A., Hedrich, S., Vasters, J., Drobe, M., Sand, W., Willscher, S., 2013. Biomining: metal recovery from ores with microorganisms. In: Geobiotechnology I. Advances in Biochemical Engineering/Biotechnology. A. Schippers, F. Glombitza and W. Sand (Eds.), Springer-Verlag, Berlin Heidelberg, pp. 1-47.

Schippers, A., Jozsa, P.-G., Sand, W., 1996. Sulfur chemistry in bacterial leaching of pyrite. Appl. Environ. Microbiol., 62(9): 3424-3431.

Schippers, A., Sand, W., 1999. Bacterial leaching of metal sulfides proceeds by two indirect mechanisms via thiosulfate or via polysulfides and sulfur. Appl. Environ. Microbiol., 65(1): 319-321.

Smith, A.M.L., Hudson-Edwards, K.A., Dubbin, W.E., Wright, K., 2006. Dissolution of jarosite $[KFe_3(SO_4)_2(OH)_6]$ at pH 2 and 8: Insights from batch experiments and computational modelling. Geochim. Cosmochim. Acta, 70(3): 608-621.

Vargas, M., Kashefi, K., Blunt-Harris, E.L., Lovley, D.R., 1998. Microbiological evidence for Fe (III) reduction on early Earth. Nature, 395(6697): 65-67.

Vera, M., Schippers, A., Sand, W., 2013. Progress in bioleaching: fundamentals and mechanisms of bacterial metal sulfide oxidation—part A. Appl. Microbiol. Biotechnol., 97(17): 7529-7541.

Wang, H., Bigham, J.M., Tuovinen, O.H., 2006. Formation of schwertmannite and its transformation to jarosite in the presence of acidophilic iron-oxidizing microorganisms. Mater. Sci. Eng. C, 26(4): 588-592.

Xia, J.-L., Yang, Y., He, H., Zhao, X.-J., Liang, C.-L., Zheng, L., Ma, C.-Y., Zhao, Y.-D., Nie, Z.-Y., Qiu, G.-Z., 2010. Surface analysis of sulfur speciation on pyrite bioleached by extreme thermophile *Acidianus manzaensis* using Raman and XANES spectroscopy. Hydrometallurgy, 100(3): 129-135.

Xia, J., Liu, H., Nie, Z., Fan, X., Zhang, D., Zheng, X., Liu, L., Pan, X., Zhou, Y., 2020. Taking insights into phenomics of microbe-mineral interaction in bioleaching and acid mine drainage: Concepts and methodology. Sci. Total Environ., 729: 139005.

Xiong, X.-X., Gu, G.-H., Ban, J.-R., Li, S.-K., 2015. Bioleaching and electrochemical property of

marmatite by *Sulfobacillus thermosulfidooxidans*. T. Nonferr. Metal. Soc., 25(9): 3103-3110.

Yang, Y., Liu, W., Bhargava, S.K., Zeng, W., Chen, M., 2016. A XANES and XRD study of chalcopyrite bioleaching with pyrite. Miner. Eng., 89: 157-162.

Yang, Y., Zhu, Z.-y., Hu, T.-t., Zhang, M.-j., Qiu, G.-z., 2021. Variation in energy metabolism structure of microbial community during bioleaching chalcopyrites with different iron-sulfur ratios. J. Cent. South Univ., 28(7): 2022-2036.

Yin, L., Yang, H.-Y., Tong, L.-L., Ma, P.-C., Zhang, Q., Zhao, M.-M., 2020. Arsenopyrite bio-oxidization behavior in bioleaching process: evidence from laser microscopy, SEM-EDS, and XPS. Front. Microbiol., 11: 1773.

Yoshida, N., Nakasato, M., Ohmura, N., Ando, A., Saiki, H., Ishii, M., Igarashi, Y., 2006. *Acidianus manzaensis* sp. nov., a novel thermoacidophilic archaeon growing autotrophically by the oxidation of H_2 with the reduction of Fe^{3+}. Curr. Microbiol., 53(5): 406-411.

Zhang, C.-G., Zhang, R.-Y., Xia, J.-L., Zhang, Q., Nie, Z.-Y., 2008. Sulfur activation-related extracellular proteins of *Acidithiobacillus ferrooxidans*. T. Nonferr. Metal. Soc., 18(6): 1398-1402.

Zhang, R., Neu, T.R., Li, Q., Blanchard, V., Zhang, Y., Schippers, A., Sand, W., 2019. Insight into interactions of thermoacidophilic archaea with elemental sulfur: biofilm dynamics and EPS analysis. Front. Microbiol., 10: 896.

Zhu, W., Xia, J.-L., Yang, Y., Nie, Z.-Y., Zheng, L., Ma, C.-Y., Zhang, R.-Y., Peng, A.-A., Tang, L., Qiu, G.-Z., 2011. Sulfur oxidation activities of pure and mixed thermophiles and sulfur speciation in bioleaching of chalcopyrite. Bioresour. Technol., 102(4): 3877-3882.

Supplemental materials for

Reductive dissolution of jarosite by inorganic sulfur compounds catalyzed by *Acidithiobacillus thiooxidans*

Hong-rui Chen[1], Duo-rui Zhang[1], Zhen-yuan Nie[1], Jin-lan Xia[1*], Qian Li[1], Rui-yong Zhang[2, 3*], He-hao Yin[1], Eva Pakostova[4]

[1]Key Lab of Biometallurgy of Ministry of Education of China, School of Minerals Processing and Bioengineering, Central South University, Changsha 410083, China

[2]Key Laboratory of Marine Environmental Corrosion and Biofouling, Institute of Oceanology, Chinese Academy of Sciences, Qingdao 266071, China

[3]Open Studio for Marine Corrosion and Protection, Pilot National Laboratory for Marine Science and Technology (Qingdao), Qingdao 266237, China

[4]Centre for Sport, Exercise and Life Sciences, Institute of Health and Wellbeing, Coventry University, Coventry, CV1 5FB, UK

* Correspondence to be addressed: jlxia@csu.edu.cn; ruiyong.zhang@qdio.ac.cn

Supplementary Figure S1. Photograph of the biosynthesized potassium jarosite (Pj)

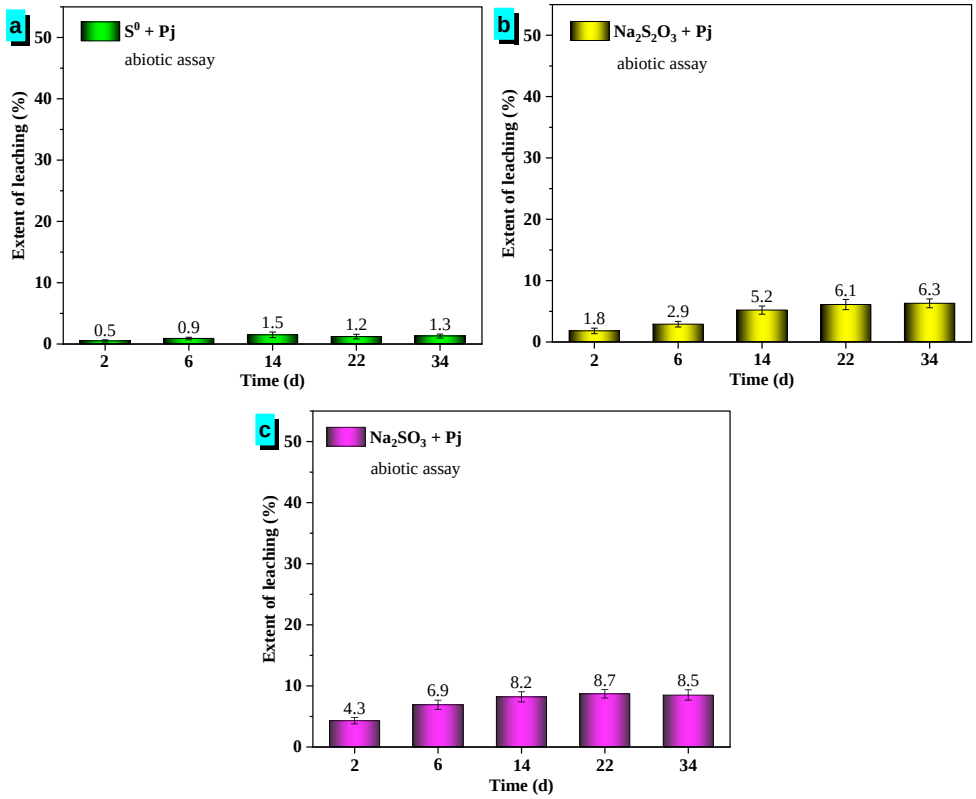

Supplementary Figure S2. Extent of leaching of Pj in the sterile controls with different inorganic sulfur compounds added. (a) S^0, (b) $Na_2S_2O_3$, and (c) Na_2SO_3.

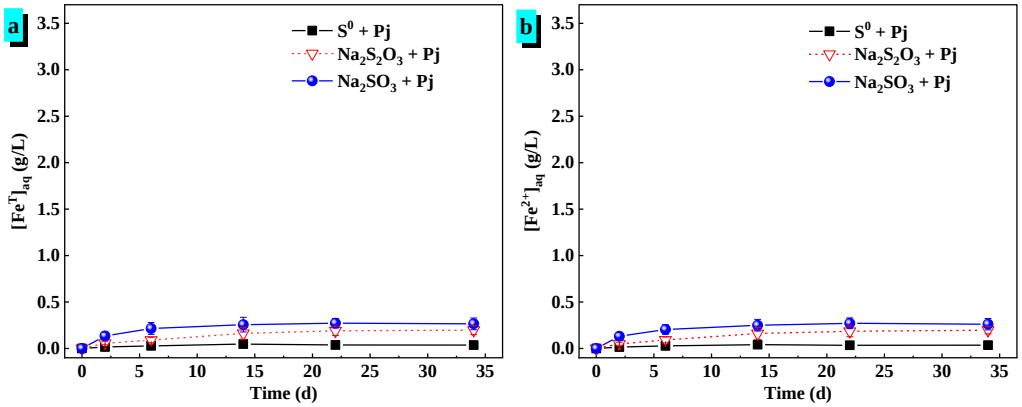

Supplementary Figure S3. Changes in (a) $[Fe^{T}]_{aq}$ and (b) $[Fe^{2+}]_{aq}$ released from Pj in the sterile controls with different inorganic sulfur compounds added.

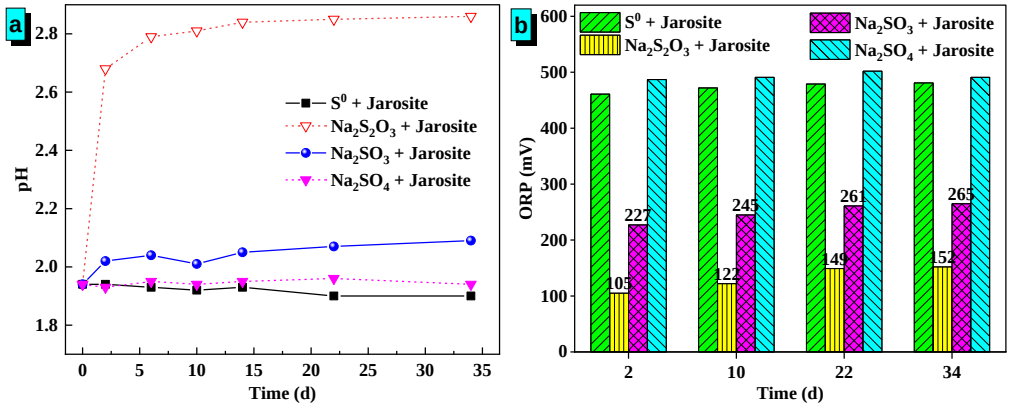

Supplementary Figure S4. Changes in solution (a) pH and (b) ORP values in the sterile controls with different inorganic sulfur compounds added.